LUND UNIVERSITY

hiPS-Derived Astroglia Model Shows Temporal Transcriptomic Profile Related to Human Neural Development and Glia Competence Acquisition of a Maturing Astrocytic Identity

Lundin, Anders; Ricchiuto, Piero; Clausen, Maryam; Hicks, Ryan; Falk, Anna; Herland, Anna

Link to publication

Creative Commons License:
CC BY-NC

hiPS-Derived Astroglia Model Shows Temporal Transcriptomic Profile Related to Human Neural Development and Glia Competence Acquisition of a Maturing Astrocytic Identity

Anders Lundin, Piero Ricchiuto, Maryam Clausen, Ryan Hicks, Anna Falk,* and Anna Herland*

Astrocyte biology has a functional and cellular diversity only observed in humans. The understanding of the regulatory network governing outer radial glia (RG), responsible for the expansion of the outer subventricular zone (oSVZ), and astrocyte cellular development remains elusive, partly since relevant human material to study these features is not readily available. A human-induced pluripotent stem cell derived astrocytic model, NES-Astro, has been recently developed, with high expression of astrocyte-associated markers and high astrocyte-relevant functionality. Here it is studied how the NES-Astro phenotype develops during specification and its correlation to known RG and astrocyte characteristics in human brain development. It is demonstrated that directed differentiation of neurogenic long-term neuroepithelial stem cells undergo a neurogenic-to-gliogenic competence preferential change, acquiring a glial fate. Temporal transcript profiles of long- and small RNA corroborate previously shown neurogenic restriction by glia-associated let-7 expression. Furthermore, NES-Astro differentiation displays proposed mechanistic features important for the evolutionary expansion of the oSVZ together with an astroglia/astrocyte transcriptome. The NES-Astro generation is a straight-forward differentiation protocol from stable and expandable neuroepithelial stem cell lines derived from iPS cells. Thus, the NES-Astro is an easy-access cell system with high biological relevance for studies of mechanistic traits of glia and astrocyte.

1. Introduction

Expansion and structural development of the primate cerebral cortex is highly associated with the emergence of the outer subventricular zone (oSVZ).[1,2] Generation and development of glia progenitor pools responsible for unique primate structures is closely linked to cellular competence and fate decision. Fetal brain development can be divided into neuro-, astro-, and oligogenesis where progenitor cells transition from being neurogenic to become gliogenic, also known as the neurogenic-to-gliogenic switch.[3] However, brain developmental features differ among species.

Invaluable information on human glia and astrocyte biology has been acquired from fetal samples, healthy tissue from surgical procedures, and post-mortem samples. Parts of human radial glia (RG) and astrocyte development are human specific. However, accessing sequential material to study brain development is limited, especially later time points of gestational and initial postnatal periods when

Dr. A. Lundin, M. Clausen, Dr. R. Hicks
Translational Genomics
BioPharmaceuticals R&D
Discovery Sciences
AstraZeneca, Gothenburg, Pepparedsleden 1, Mölndal 431 83, Sweden

Dr. P. Ricchiuto
Data Sciences and Quantitative Biology
Discovery Sciences, R&D
AstraZeneca, Darwin Building, 310 Milton Rd, Cambridge CB4 0WG, UK

The ORCID identification number(s) for the author(s) of this article can be found under https://doi.org/10.1002/adbi.201900226.

Prof. A. Falk, Prof. A. Herland
Department of Neuroscience
Karolinska Institutet
Stockholm 17177, Sweden
E-mail: anna.falk@ki.se; aherland@kth.se

Prof. A. Herland
Division of Micro and Nanosystems
KTH Royal Institute of Technology
Stockholm 10044, Sweden

Prof. A. Herland
AIMES
Center for the Advancement of Integrated Medical and Engineering Sciences
Karolinska Institutet
Stockholm 17177, Sweden

glia and astrocyte cellular identities progress. Human-induced pluripotent stem cell (iPSC) technology provides a source of human cells useful for investigating mechanisms linked specifically to human biological traits. We and others have developed protocols to generate human iPSC derived astrocytic models,[4,5] which display characteristic astrocytic features including SLC1A3 driven glutamate uptake,[4] inflammatory response,[6] and calcium propagation in response to ATP[7] and glutamate stimulation.[4,8] Additionally, we have previously shown that neurogenic long-term neuroepithelial stem (ltNES) cells develop into neurons,[9] which together with the ltNES-derived Astroglia (NES-Astro) model demonstrate the functional neurogenic and gliogenic developmental programs of ltNES cells. However, a detailed temporal study of human iPSC derived astroglia differentiation to investigate the relevance and model translatability of human specific glia development traits has not been performed.

Higher diversification of progenitors and extended neurogenic period in higher primates likely require additional cell competence regulation to timely differentiate into neurons and later astrocytes. The regulatory mechanism responsible for the diversification and maintenance of the proliferative capacity among glia progenitors in higher primates have been related to a more complex control of cell cycle.[1] It is hypothesized that expansion of regulatory networks is related to the evolutionary increase in number of non-coding RNAs (ncRNAs) along the phylogenic tree,[10] more specifically long non-coding RNAs (lncRNAs), and micro RNAs (miRNAs) due to their highly dynamic changes during evolution.[1]

With increasing brain complexity, the long evolutionary relationship between neurons and glia has by selective pressure diversified glia biology to likely meet the needs of neuronal sub-types.[11] The additional developmental phase of the oSVZ and supragranular expansion possibly provide different settings for astroglia generation. How this affects human astrocyte diversity remains elusive. Transcriptomic analysis displays a lesser evolutionary conservation of glia/astrocyte-associated genes compared to neuron-associated genes.[12] Rodent and human share transcriptomic profiles across species where commonly astrocyte associated genes ALDH1L1, AQP4, GFAP, GJB6, GLUL, SLC1A2, and SLC1A3 are enriched in both rodent and human astrocytes. However, only 30% of human astrocyte enriched genes are enriched in mice, and 52% of mouse astrocyte enriched genes are enriched in human.[13]

Transcript analyses of different human brain regions from adult[14] and fetal brain[15] reveal distinct and vast diversity of neuronal sub-types. However, the number of transcriptomic signatures of astrocytic subtypes does not match the morphological classification,[16] seemingly not to capture the evolutionary divergence of human glia biology. However, the accelerated organization of the human prefrontal cortex is not exclusively associated to neuronal specific transcriptomic profiles defining cortical layers but also associates to astrocyte-specific genes.[17] Development of cortical structure during neurogenesis seemingly affect subsequent astrocyte sub-specification resulting in morphological and molecular differences.[18] Several studies have characterized astrocytic subtypes,[19–21] but if these subclasses display significant transcriptomic or functional differences is poorly understood. Moreover, it has been shown that

human astrocytes are larger, structurally more complex, and demonstrate faster calcium propagation compared to rodent counterparts. Moreover, higher primates and humans display species specific astrocytic subtypes.[16] In addition, transplanted human glia progenitors, which differentiate into human astrocytes in vivo, lead to increased cognitive function in mice,[22] indicative of cell-intrinsic functional differences.

Herein we study the temporal transcriptional change of the NES-Astro model to investigate if it recapitulates features of human brain development. We evaluate the transcriptomic coverage comparable to samples derived from fetal brain samples, including ncRNA profiles. Specifically, we study how the temporal transcriptomic profile is associated to brain development and cellular transcript identities for neurons, intermediate progenitors, ventral- and outer RG as well as astroglia.

2. Results

2.1. Wide Transcriptome Coverage of RNA Species in NES-Astro Differentiation

We have previously shown associations of iPSC derived ltNES cell differentiation to early neural development (GW6-12).[9,23,24] Here we wanted to investigate if directed glia differentiation[4] could capture temporal transcriptional patterns of glia and astrocyte development. To generate a timeline association to embryonic development sequential samples were isolated during 28-days of directed glia differentiation capturing the transition from NSC to astroglia phenotype (**Figure 1**A). To validate the bioinformatic processing of sequencing data we assessed the total transcriptional coverage by investigating the diversity distribution of RNA species including mRNA and lncRNA (Figure 1B) which displayed similar profile as previously reported of primary human fetal brain tissue.[25] Principle component analysis revealed distinct separation between the directed glia differentiation and the undifferentiated control culture at all four timepoints (Figure 1C). Moreover, the PC1 component separates samples dependent on differentiational time points (Figure 1C) demonstrating a clear transcriptional change over time.

Overall, transcriptomic coverage of mRNA and ncRNA are in line with previous studies of embryonic brain development[25] up to GW23, here leading to an astrocytic phenotype over the differentiation of 28 days.[4]

2.2. High Abundance Transcriptomic Clusters Relate to Brain Development and Cell Identity Transition

To investigate transcriptomic patterns over differentiation time points, we across cell lines, performed model-based cluster analysis to characterize genes based on their abundance profiles (best performing model of 12 cluster guided by Bayesian information criterion index, same across cell lines).[26–29] Consistently for each cell line we identify two clusters that have the highest differentially expressed transcripts, these contained a higher number of known glia associated markers (Table S1,
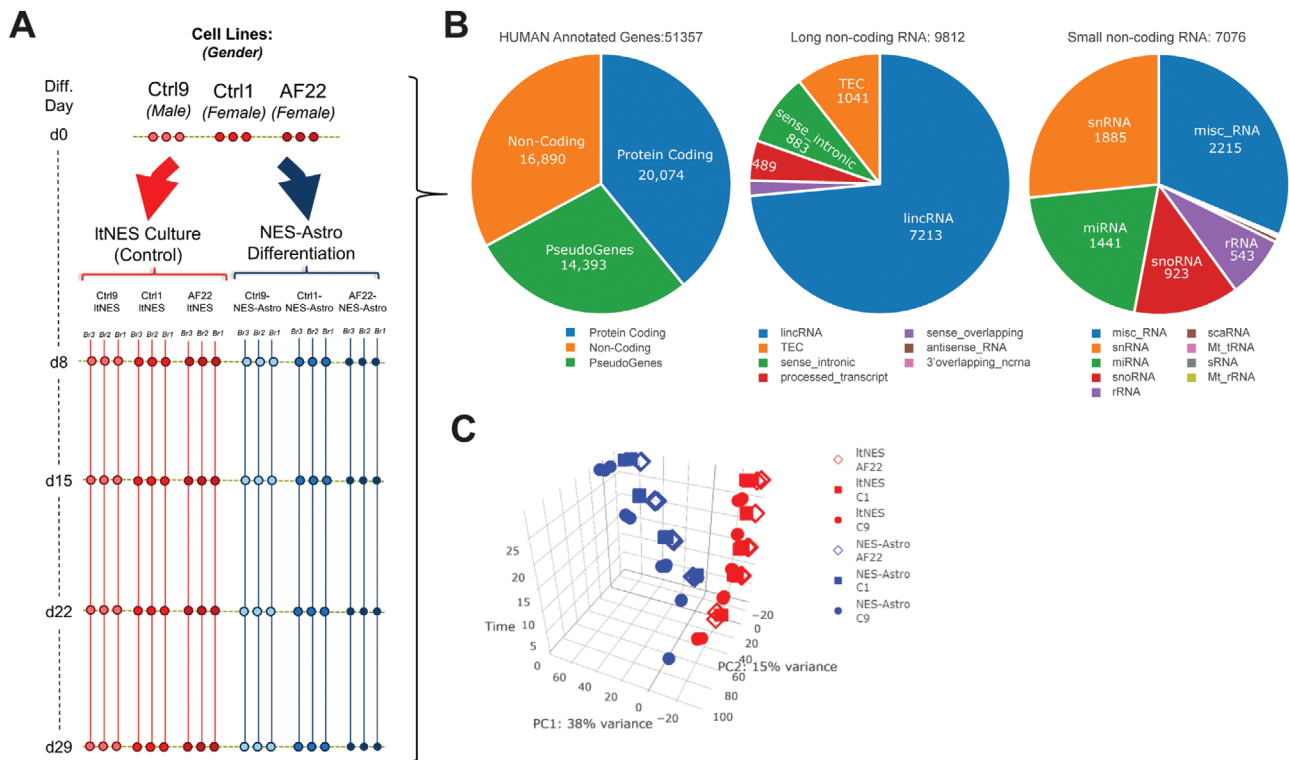
Figure 1. Transcriptional overview of directed glia differentiation of three independent cell lines (Ctrl1, Ctrl9, AF22). A) Schematic overview of RNA sampling during NES-Astro differentiation with time matched controls. Initially, three individual ltNES cell cultures of each line (Ctrl9, Ctrl1, AF22) are at d0 split into differentiation and control maintenance cultures, which are used as time matched RNA normalization controls. Control and differentiation cultures contain three individual cultures of each line, respectively, in total 18 cultures. These are sampled each timepoint generating 81 RNAseq samples in total across the directed differentiation of 29 days. Sequencing reads (fastq) were aligned via Hisat2 (hg38), and read counts were annotated using Sailfish and Htseq-count. Count level were normalized to the time match control cell line and used for differential expression analysis (DESeq2). B) Visual representation of the transcript annotation across the 81 RNA samples. C) A principal components analysis on DESeq2 rlog transformed data of the 81 RNA samples including each cell line and replicate at differentiation and control time points day d0, d8, d15, d22, d29. Data shown from three independent experiments of three independent cell lines, $n = 9$, at both differentiation and control conditions. C1 = Ctrl1, C9 = Ctrl9, Br = Biological replicate.

Supporting Information). Using gene set enrichment analysis,[30] we can show that these clusters display clear association to brain, neural cell biology, and development (**Figure 2**A,B). Interestingly, these clusters also related to circadian, ECM, integrin, and Alzheimer's disease-presenilin pathways (Figure 2C) as previously observed in developmental studies of human and primate associated transcriptional traits.[31,32]

To relate these transcriptomic associations to cellular development, we then investigated temporal patterns of cell type specific transcripts in glia selected clusters (Figure 2D).[13,31,33–39] Indeed, we could identify neuronal and astrocyte type specific markers in these clusters including neuron (*DCX, RELN, NCMA1*) and intermediate progenitor (*NEUROD1, NEUROD4, ELAVL4*), pan-RG (*FOS, EGR1, HES1*), ventral RG (*FBXO32, PROM1*), outer RG (*MOXD1, FAM107A, TNC*), and astroglia (*ALDH1L1, SOX9, CA2*) (Figure 2E). Moreover, temporal patterns of cell identity markers related to neuronal and intermediate progenitors display short peaked expression across one to two time points followed by downregulated expression. This in contrast to ventral-, outer-RG, and astroglia marker profiles which after expressional increase at d8 and onward, depending on marker, sustained high expression overtime together with an accumulating number of cell-specific markers (Figure 2F).

In summary, the gene clusters with the highest temporal differential expression in NES-Astro differentiation are heavily associated to brain development and human developmental features including transcriptional cell type identities. Moreover, the accumulation and sustained expression of glia markers highlight the transition of a maturing and expanding glia population during our directed differentiation.

2.3. Common Gliogenic Proteomic Markers Demonstrate a Competence Switch

Next, to validate the observed temporal transcriptomic transition to glia we investigated protein translation of key glia developmental markers. Immunostaining patterns of NFIA and SOX9 (**Figure 3**A,B) corroborated transcriptional expression, demonstrating the presence of proteins important for glia developmental competence.[40–43] Further investigation of brain developmental events by FABP7 expression, marking RG expansion in the SVZ at GW13[2] and further enriched in the oSVZ at GW16,[31] demonstrated an increasingly strong and homogenous populational expression over time. Moreover, in line with developmental time lines, SLC1A3, enriched
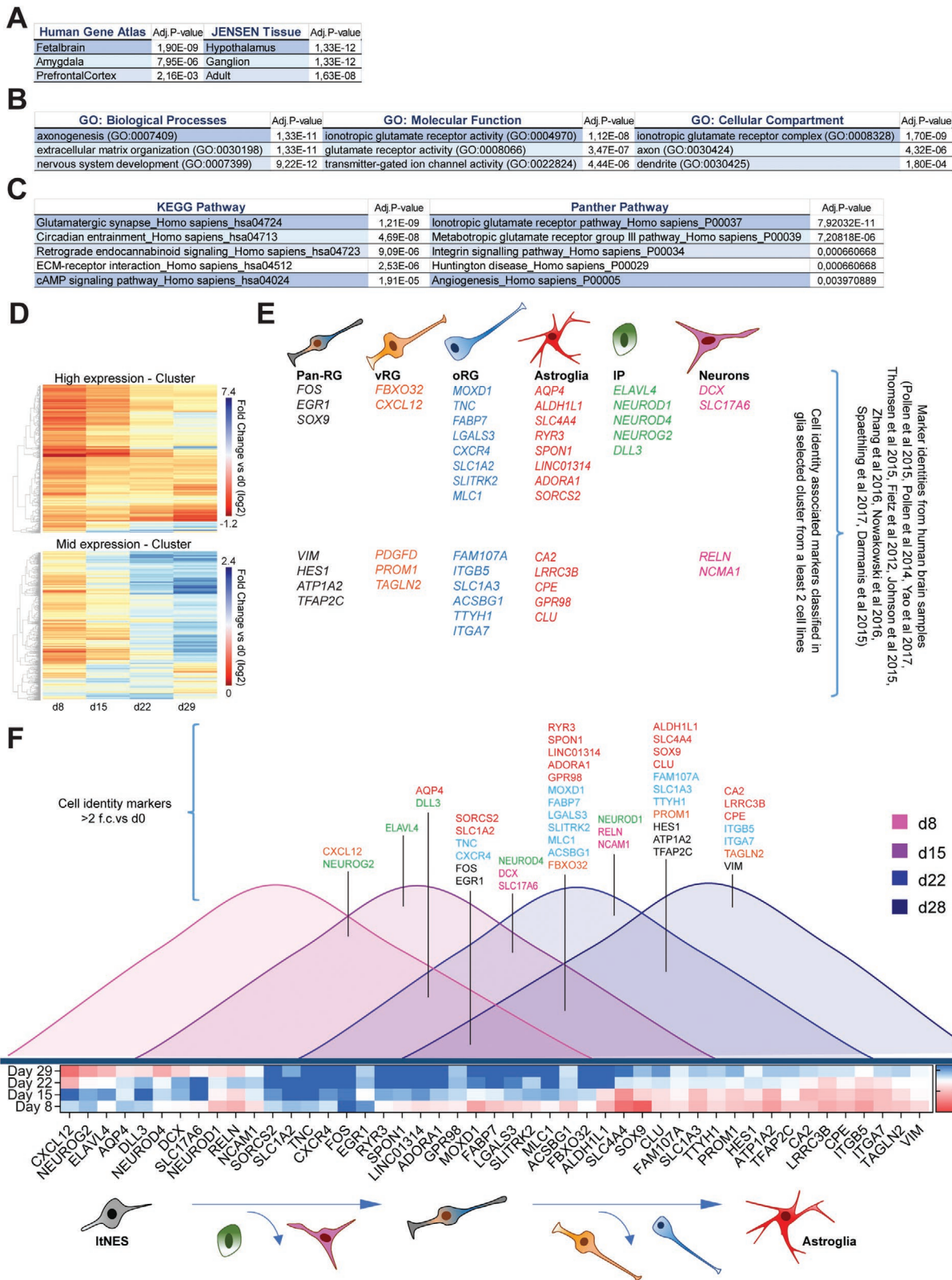
ADVANCED
SCIENCE NEWS
www.advancedsciencenews.com

ADVANCED
BIOSYSTEMS
www.adv-biosys.com

A

Human Gene Atlas	Adj.P-value	JENSEN Tissue	Adj.P-value
Fetalbrain	1,90E-09	Hypothalamus	1,33E-12
Amygdala	7,95E-06	Ganglion	1,33E-12
PrefrontalCortex	2,16E-03	Adult	1,63E-08

B

GO: Biological Processes	Adj.P-value	GO: Molecular Function	Adj.P-value	GO: Cellular Compartment	Adj.P-value
axonogenesis (GO:0007409)	1,33E-11	ionotropic glutamate receptor activity (GO:0004970)	1,12E-08	ionotropic glutamate receptor complex (GO:0008328)	1,70E-09
extracellular matrix organization (GO:0030198)	1,33E-11	glutamate receptor activity (GO:0008066)	3,47E-07	axon (GO:0030424)	4,32E-06
nervous system development (GO:0007399)	9,22E-12	transmitter-gated ion channel activity (GO:0022824)	4,44E-06	dendrite (GO:0030425)	1,80E-04

C

KEGG Pathway	Adj.P-value	Panther Pathway	Adj.P-value
Glutamatergic synapse_Homo sapiens_hsa04724	1,21E-09	Ionotropic glutamate receptor pathway_Homo sapiens_P00037	7,92032E-11
Circadian entrainment_Homo sapiens_hsa04713	4,69E-08	Metabotropic glutamate receptor group III pathway_Homo sapiens_P00039	7,20818E-06
Retrograde endocannabinoid signaling_Homo sapiens_hsa04723	9,09E-06	Integrin signalling pathway_Homo sapiens_P00034	0,000660668
ECM-receptor interaction_Homo sapiens_hsa04512	2,53E-06	Huntington disease_Homo sapiens_P00029	0,000660668
cAMP signaling pathway_Homo sapiens_hsa04024	1,91E-05	Angiogenesis_Homo sapiens_P00005	0,003970889

Figure 2. Model-based cluster analysis. Aligned (Hisat2 to hg38) read counts (Sailfish and Htseq-count) were normalized to time match controls samples for model-based clustering. Based on transcriptomic pattern did model-based cluster analysis generate 12 different clusters. Common glia markers (Table S1, Supporting Information) were initially used to identify clusters associate with glia biology. The two clusters containing the highest number of glia markers in each cell line (in total 6 clusters) were analyzed by gene set enrichment analysis;[30] A) Human Gene Atlas and Jensen tissue,
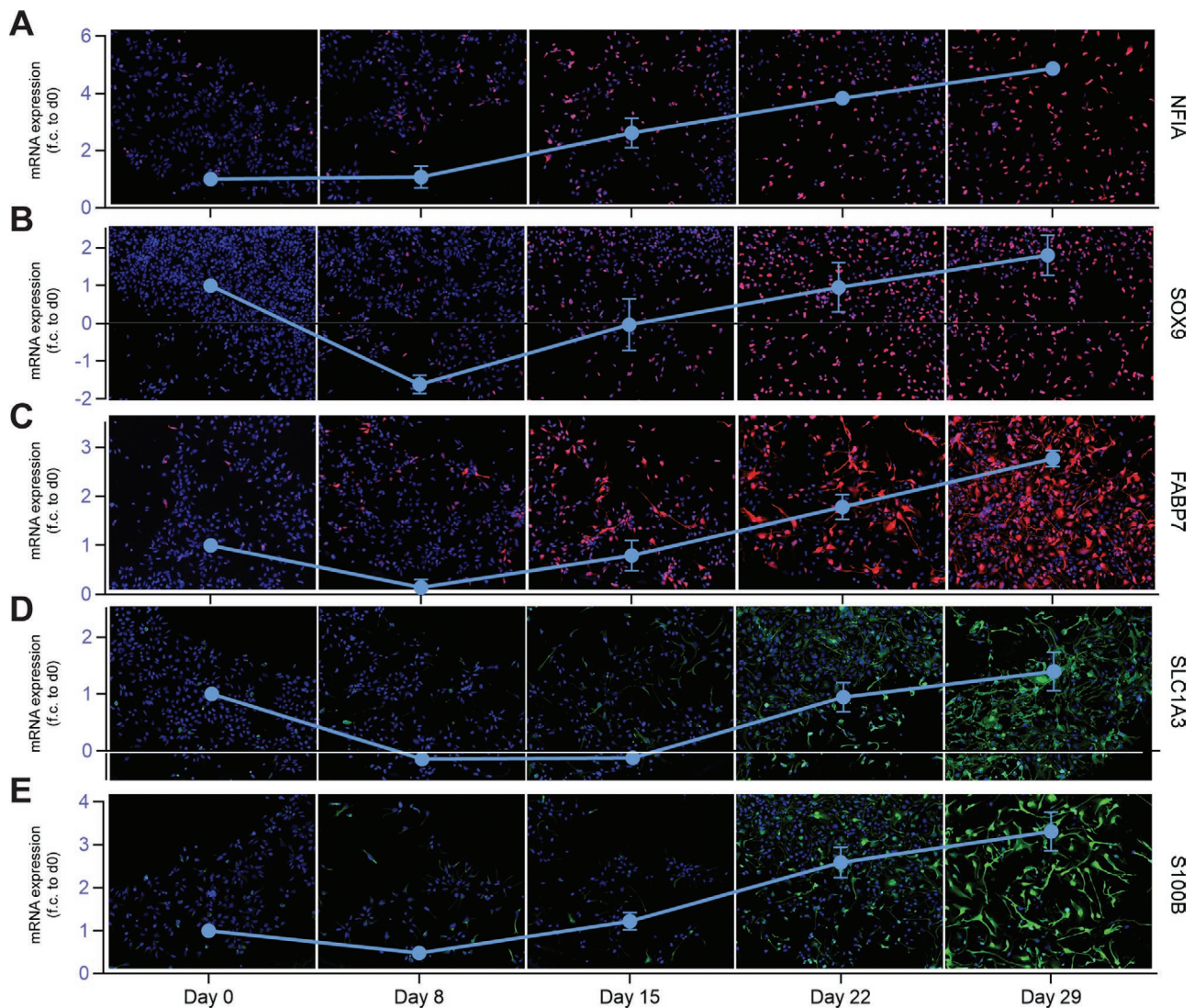
**ADVANCED
SCIENCE NEWS**

www.advancedsciencenews.com

**ADVANCED
BIOSYSTEMS**

www.adv-biosys.com

Figure 3. Expression of gliogenic markers during NES-Astro differentiation. Expression levels of mRNA as blue graphs overlaying protein expression are shown for A) NFIA, B) SOX9, C) FABP7, D) SLC1A3, and E) S100B. Transcriptomic expression level derived from model-based cluster values. RNA data are derived from three replicates of each individual cell line (AF22, C1, and C9), in total $n = 9$. Data shown as mean ± SEM. Protein expression is shown for cell line C1. Similar protein expression is observed for AF22 and C9 (data not shown).

in human oSVZ at GW16[31] but also expressed in later astroglia,[20] showed homogenous staining across the cell population (Figure 3D) one time point later compared to FABP7. Additionally, S100B, a gene associated to astrocytic fate in the cerebral cortex[44] had similar pattern as SLC1A3, with strong expression in later time points (Figure 3E).

Together, the protein expression demonstrates a developmental timeline capturing stemness loss of the NSC while a competence change results in an accumulating glia and astroglia identity.

2.4. Known Gliogenic miRNAs Govern NES-Astro Differentiation

ncRNAs have become recognized as an important aspect of transcriptional and translational regulation to control cellular states and developmental progression.[45–47] We therefore investigated the transcriptomic patterns related to ncRNA and found that a subset of the highest differentially expressed genes were related to miRNA metabolic processes (GO:0010586) including LIN28A/B, associated to regulation of gliogenesis.[48] Since pri-microRNA not directly correlate to mature miRNA[46] we

B) GO-term enrichment, C) pathway analysis. Enrichment scores are calculated by Fisher's exact test proving output ranking by adjusted p-value. D) Representative heatmaps of glia associated clusters of C1 NES-Astro differentiation. E) Cell identity markers of Pan-RG, vRG, oRG, astroglia, IP, and neurons present in glia associated clusters identified in at least two out three cell lines. F) Venn-diagram visualized as time showing at what time point identity markers have a greater than twofold expression compared to d0. Heatmap of the markers presented in the Venn-diagram shown as fold change compared to d0, based on model-based clustering values. RG: radial glia, vRG: ventral RG, oRG: outer RG, IP: intermediate progenitor, ltNES: long-term neuroepithelial stem cells.
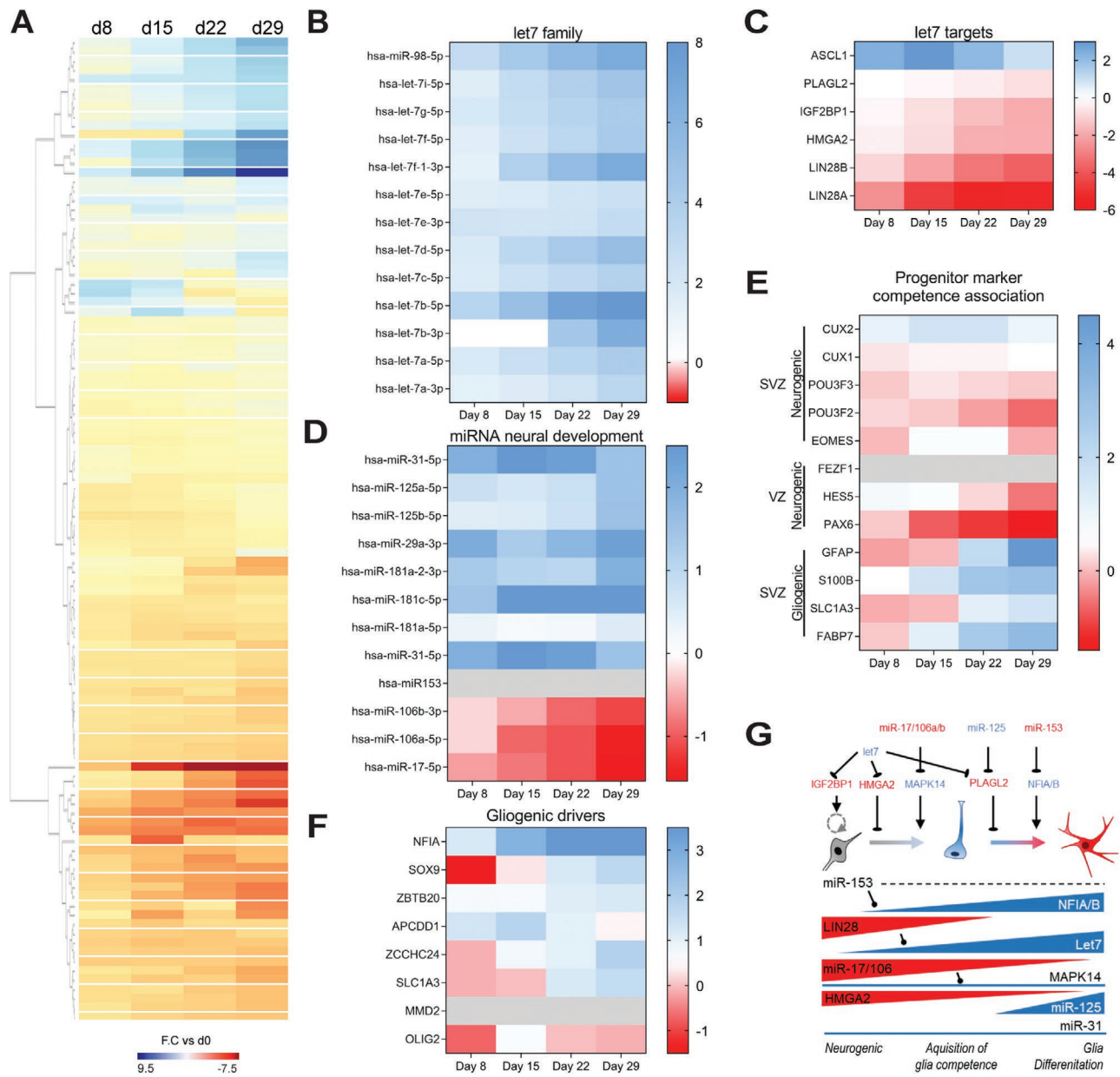
Figure 4. MicroRNA expressional patterns. Sequencing reads (fastq) were analyzed using SeqBuster.[73] A) miRNA expression heatmap of mature miRNAs detected in AF22 NES-Astro across differentiation time points d8, d15, d22, and d29. Temporal transcript patterns of B) Let-7 family members and C) known targets and downstream effectors. D) Heatmap of temporal miRNA expression patterns related to the neurogenic-to-gliogenic switch. E) Marker competence expression profiles related to progenitor cell fate development.[52] F) Expression pattern of gliogenic drivers. G) Schematic summary of temporal transcript expression patterns related to the neurogenic-to-gliogenic switch. Model schematic adapted from ref. [3]. Downregulated transcripts in red and upregulated transcripts in blue. Dotted line: non-detected transcript. Samples are derived from five timepoints; day 0, 8, 15, 22, and 29. Transcriptomic expression levels of longRNA from model-based clustering are derived from 3 replicates of each individual cell line (AF22, C1, and C9), in total $n = 9$. Transcriptomic data of miRNAs are derived from three replicates of one individual cell lines (AF22). Data is shown as fold change relative d0.

performed miRNA sequencing across the differentiation time points (**Figure 4**A) to investigate the association between gene expression and ncRNAs in relation to the cell differentiation progression. We observed that several let-7-family miRNAs, directly targeting LIN28A/B,[48] were included in the most temporally differentially expressed miRNAs (Figure 4B). As let-7/ LIN28B has been suggested to regulate gestational progression

of the developing human brain[48] we investigated expression patterns of downstream effectors and found significant regulation of *HMGA2, IGF2BP1, PLAGL2, HES5, USP44* (Figure 4C). Moreover, we could corroborate several transcriptional trends important for developmental progression of NSC[3] including downregulation of miR-17/106a/b, miR-153 together with upregulation of astroglia associated transcripts

such as miR-31-5p, miR-181a-5p/a-2-3p/c-5p, miR-29a-3p, miR-125a/b (Figure 4D).[49–51] These miRNA trends are accompanied with temporal gene expression profile favoring gliogenic cell progression with weaker neurogenic profile (Figure 4E).[52] Early gliogenic induction is govern by NFIA and SOX9[40] of which astrocyte associated Apcdd1, Zcchc24, and oligodendrocyte associated Mmd2 target genes can rescue Glast and Fgfr3 or Glast, Fgfr3, and Olig2 expression respectively.[40] Our temporal transcript profile shows increased expression of APCDD1, ZCCHC24, SLC1A3 as OLIG2 and MMD2 are decreased or absent, respectively (Figure 4F). Moreover, we also observe an increase temporal expression of ZBTB20 (Figure 4F) which has been shown to act in parallel with NFIA and SOX9 to drive astrogenesis.[53]

In conclusion, an investigation of temporal patterns of long and short RNAs during directed glia differentiation provides a unique network association of developmental regulation. The importance of miRNA regulation has been increasingly recognized in multiple biological contexts. However, our results are one of the few showing the importance of miRNAs affecting gene expressional patterns during NSC specification and glia development in vitro (Figure 4G).

2.5. NES-Astro, a Model to Study Human-Specific Features of Gliogenesis

Expansion of the human oSVZ[2] and subsequent astroglia development[54] associates to regulatory mechanisms accounting for the divergence in developmental architecture compared to other mammals.[1] To provide alternatives for the limited access to primary material to study human specific traits, we investigated if these developmental processes were captured in our transcriptomic profiles in the NES-Astro differentiation.

Outer RG contribute to brain expansion[1] by sustaining a proliferative niche.[33] We observed that highly differentially expressed genes over the NES-Astro differentiation had a strong association to extracellular matrix organization (GO:0030198) (Figure 2B,C), recently identified to be important for human neocortex expansion as opposed to reports of mouse development.[31] Genes include *TNC*, *ITGB5*, *SDC3*, *HS6ST1*, and *LIFR* which have been suggested as mechanistically important in this process.[33] Moreover, we detected trophic factors *PDGFD* and *BMP7* shown to be enriched in human RG compared to mouse[25,33] and suggestive to be part of regulating the RG proliferative niche together with STAT3 signaling (**Figure 5**A).[33]

Gliogenic competence onset is dependent on FGF signaling regulating MEK/ERK signaling via *ETV5* expression,[55] which is enriched in human outer RG.[33,36] Human neocortical transition of apical RG to outer RG can be induced by FGF-ERK-ETV signaling, observed to be more dominant in human than in mice apical RG.[56] We detected high upregulation of *ETV5* together with human outer RG identity markers (*MOXD1*, *FAM107A*, *LGALS3*, *TKTL1*) not expressed in mouse RG (Figure 5A).[33] Additionally, we observed temporal increase of outer RG enriched markers (*TNC*, *ITGB5*, *ACSBG1*) associated with astrocytes later in development (Figure 5B).[33] However, in contrast to neurogenic outer RG which strongly express *NOG* to inhibit BMP signaling[33] we detected downregulation of *NOG* over time accompanied by increased levels of *BMP2* and *BMPR2* (Figure 5E).

Recently, a human specific lncRNA called lncND (antisense of TCONS_00003534) was identified and observed to be enriched in RG of the VZ and oSVZ but faintly expressed in the cortical plate and differentiated neurons.[57] LncND act as a sponge for miR-143-3p and regulate the expression of notch receptors and notch signaling which affect RG expansion.[57] We could detect temporal downregulation of miR-143-3p with
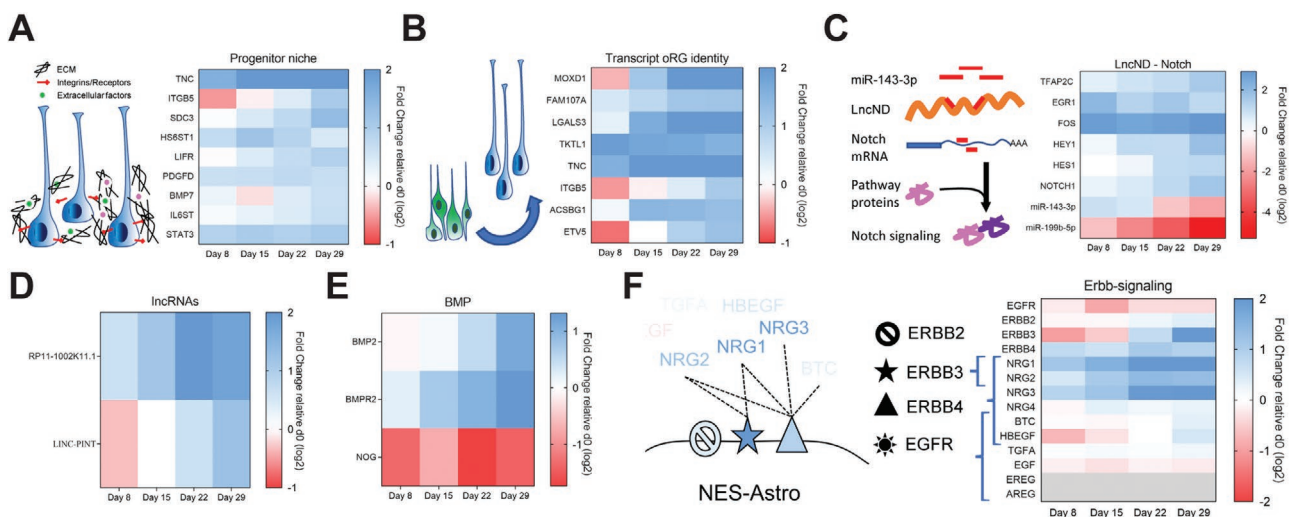

Figure 5. Transcription profiles of proposed mechanism related to human brain development. A) Components of the stem cell niche driving oRG expansion. B) oRG transcript identity. C) Transcripts related to a human specific lncRNA, lncND, enriched in the VZ and oSVZ. D) Long ncRNA associated to RG identity. E) BMP associated transcripts. Samples are derived from five timepoints; day 0, 8, 15, 22, and 29. F) Expressional pattern of Erbb-signaling receptors and modulators across differentiation time points. Transcriptomic expression levels of longRNA from model-based clustering are derived from 3 replicates of each individual cell line (AF22, C1, and C9), in total *n* = 9. Transcriptomic data of smallRNA (miRNAs) are derived from three replicates of one individual cell lines (AF22). Data is shown as fold change relative d0.

**ADVANCED
SCIENCE NEWS**
www.advancedsciencenews.com

**ADVANCED
BIOSYSTEMS**
www.adv-biosys.com

upregulation of *NOTCH1* (Figure 5C) and associated genes *HES1* and *TFAP2C*. Notch target genes *FOS* and *EGR1*, rarely detected in mouse and ferret but specific for human RG,[34] shared similar upregulated expression profiles in our data. Additionally, miR-199b-5p, a *HES1* target gene, displayed a very strong temporal downregulation. Moreover, in relation to increased regulation of proliferation via ncRNAs[1] we could observe increased expression of lncRNAs *RP11-1002K11.1* and *LINC-PINT (LOC646329)* (Figure 5D), demonstrated to regulate proliferation[25] and identified to be enriched in human RG (GW13-23).[25,37]

Notch signaling and ERBB receptors are related to RG expansion and cell transition into astrocytes.[33,37,58,59] In contrast to EGFR, ERBB2, and ERBB4 expression in mouse human astrocytes do also express ERBB3.[60] We could observe strong upregulation of *ERBB3* expression compared to *EGFR*, *ERBB2*, and *ERBB4* (Figure 5F). Moreover, miR-143-3p, target human specific lncND[57] has a predicted 8mer target for *ERBB3* (TargetScan) which showed an anticorrelating expression pattern (Figure 5F).

In summary, several temporal transcriptomic patterns associated to sustained proliferative niches and signaling pathways driving RG development can be observed during NES-Astro differentiation.

2.6. Astrocytic Fate

To relate the proliferative niches of RG and its cellular transcript identities to astrocyte development we finally investigate similarities between our temporal transcriptomic profiles with already analyzed astrocytic data sets of primary and PSC organoid isolated astrocytes.[13,61] It has been suggested that RG transition from neurogenic to astrogenic occurs between GW15-35,[54] concurring with oSVZ expansion and outer radial glia (oRG).[2] We could observe high temporal increase of *TNC*, *ACSBG1*, and *MOXD1* (Figure 5B), outer RG enriched transcripts which overlap with astroglia cell fate.[33] Moreover, we could conclude that common astrocytic gene expressed in mouse and human[13] *GFAP, ALDH1L1, AQP4, CLU, SLC1A2, SLC1A3, SLC4A4, ELOVL2, ACSBG1, TTYH1, ATP1B2, SOX9* could also be identified in the glia marker selected clusters (**Figure 6**A) together with human astrocyte enriched genes and lncRNAs; *FAM198B, RYR3, AMY2B, ALDH1L1, SLC1A2, CPE, LRRC3B, GPR98, LINC01314, LINC00152, UG0898H09*[2,13,38] (Figure 6B). Furthermore, focusing on human-enriched adult astrocytic transcripts showed small overlap of top ranked astrocytic classifiers[13,38,39] (Figure 6D). Comparison of the temporal expression did not show a uniform expression to any specific astrocytic classifier lists but a broad expression of markers across all three studies (Figure 6D).

To further investigate RG transition to an astrocyte identity, we compared our dataset to expression patterns of brain organoid models.[61] Isolated glia from brain organoids revealed three main clusters; 1, 2, and 3, identifying with VZ progenitors and fetal astrocytes,[61] outer RG,[33] and mature astrocytes,[13,39] respectively. We could observe expression of 144 out of the 150 genes, top 50 genes of each cluster. Temporal expression over the differentiation time points showed a decreased association

to VZ progenitors in contrast to increased association to oRG and mature astrocyte identity (Figure 6D,E). Moreover, we could observe an increase in organoid astrocyte populational markers *AQP4, ALDH1L1, RANBP3L,* and *IGFBP7*[61] together with SLC1A2 transcript and protein expression (Figure 6F). Together, this comparison show that the NES-Astro model capture transcript expressional profiles observed in organoid models and in vivo. Together with a significant drop in proliferation,[4] as observed in adult like astrocytes,[13,61] the functional profile[4] and temporal transcriptomic and protein expression of the NES-Astro model associate with feature of mature astrocytes.

3. Discussion

Investigation of mechanistic features responsible for evolutionary diverged RG expansion of the cerebral cortex and developed complexity of astrocytes require human models with good translatability. The drivers initiating gliogenesis and progression toward an astrocytic cell fate and acquisition of astrocytic function are still poorly understood. Here we show, by studying cellular populational development, that ltNES cells undergo neurogenic-to-gliogenic competence change during directed astroglia differentiation. The change does not occur in all cells at the same time but in each cell individually based on intrinsic programs in relation to extrinsic factors. An increasing fraction of cells will acquire a gliogenic and observed as a switch when enough cells become gliogenic. Protein and transcript profiles including both long- and small RNAs corroborate current proposed mechanistic models governing gliogenic competence in humans. Furthermore, temporal transcriptomic traits of the NES-Astro model show an increasing RG transcript identity over time, displaying proposed mechanism for maintaining proliferative capacity of the outer RG population responsible for expansion of the oSVZ. Finally, the NES-Astro converges into an astroglia/astrocyte population at the end of the differentiation period, acquiring key markers and association to mature astrocytic transcript profiles.

Cerebral organoid culture models can capture important developmental features of neurons and astrocytes.[61–63] However, methods are labor intensive and analytically complex to investigate. Recent progress has reduced derivation time of directed human iPSC derived astrocytes drastically from months[5] to weeks.[4] Alternative methods using overexpression of transcription factors NFIA, NFIB, and SOX9 in combination with astrocytic differentiation media has also been shown to quickly generate astrocytes from human PSC,[41–43] previously shown difficult to generate from human fibroblasts.[64] This might indicate the necessity of a favorable epigenetic state for NFIA and SOX9 to activate gliogenic development; we can show the onset of NFIA and SOX9 mRNA and protein expression by simple directed differentiation using a stable neurogenic stem cell precursor, ltNES cells.

Moreover, we observe that temporal transcriptomic patterns of mRNA and miRNA follow proposed models of neurogenic-to-gliogenic switch in neural progenitors, including regulation of epigenetic state.[3] MicroRNA biogenesis via LIN28A in relation to let-7 expression has been shown to have a central role in glia competence acquisition, regulating chromatin protein
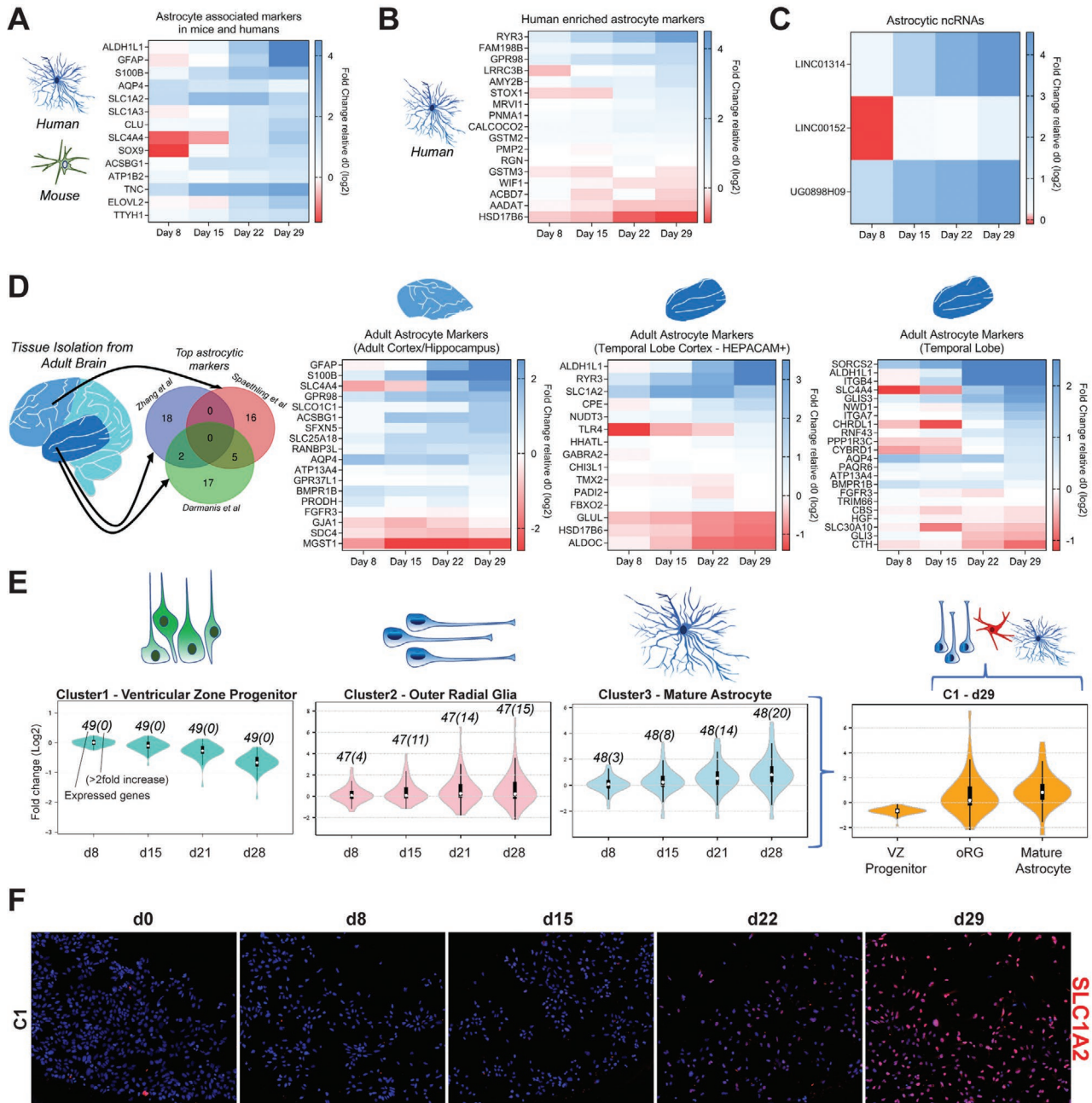
**ADVANCED
SCIENCE NEWS**

www.advancedsciencenews.com

**ADVANCED
BIOSYSTEMS**

www.adv-biosys.com

Figure 6. Glia development acquiring astrocyte identity. Temporal expression of transcripts associated to A) common astrocytic markers expressed in both mouse and human,[13] B) top human enriched astrocytic markers compared to mice,[13] and C) astrocytic associated ncRNA.[2,38] D) Venn diagram of human adult astrocyte top 20 enriched transcripts identified from primary cell isolation of human cortex,[38] temporal lobe cortex,[13] and temporal lobe[39] which are expressed in the NES-Astro model. E) Violin plots of NES-Astro temporal transcript expression of gene clusters 1, 2, and 3 associated to with VZ progenitors and fetal astrocytes, oRG and mature astrocytes, respectively.[61] Individual values: number of expressed transcripts (transcripts having a greater than twofold increase compared to d0). Highlighting NES-Astro transcript expression at day 29 of gene clusters 1, 2, and 3. F) Immunocytochemical staining of SLC1A2 across differentiational time points. Transcriptomic expression levels of longRNA from model-based clustering are derived from three replicates of each individual cell line (AF22, C1, and C9), in total n = 9. Transcriptomic data of smallRNA (miRNAs) are derived from three replicates of one individual cell lines (AF22). Data is shown as fold change relative d0.

HMGA2 and notch effector HES5 driving developmental progression and gliogenesis.[48] We assume that since there was no detectable level of miR-153, otherwise hindering NFIA/B expression,[3] together with neurogenic fate restriction by the downregulation of miR-17/106a/b[47] the miRNA expressional profile allows for further glia specification.

Based on panRG and oRG markers FABP7 and SLC1A3,[2,33,37,61] we demonstrate by temporal transcript and

protein expression NSC to RG transition. Recent studies have highlighted specific mechanisms linked to RG development in humans. In our data we can identify associated genes to mechanisms for maintaining stemness of outer RG in the oSVZ including ECM regulation,[31] local trophic factor production, active LIFR/STAT3 signaling pathways,[33] and notch signalling.[65] Moreover, we observe transcriptomic patterns in line with recently discovered human specific lncRNA, lncND, downregulating miR-143 expression, and mediating notch signaling via *HES1* and *HEY1*[57] affecting RG enriched downstream targets *FOS, EGR1*, and *TFAP2C*.[34] Together with oRG trophic factors *PDGFD* and *BMP7*,[33] enriched RG lncRNAs[25,37] this indicate that the NES-Astro model captures mechanistic features associated to the evolutionary developed oSVZ and human brain expansion.[1]

Astrocyte generation is initiated subsequently to the second wave of neurogenesis by RG cells.[2,54,66] Here we detected that outer RG transcriptomic cellular identity is accompanied by transcripts associated with astroglia (SOX9, GFAP, SLC1A2, SLC1A3), human enriched astrocyte markers (KCNJ10, RYR3, ALDH1A1, AMY2B, GPR98, LRRC3B),[13] and mature astrocytic markers (ALDH1L1, AQP4, RANBP3L, IGFBP7, RYR3).[13,61] Moreover, we observe a temporally increased expression of astrocyte-associated S100B and SLC1A2[20,44,67] which together with astrocytic functional acquisition[4] demonstrate development of an astrocyte identity.

Human astrocytes both display functional and subtype heterogeneity not observed in rodents.[68] In addition, human brain development shows specific features of oSVZ expansion.[2,33] If human astrocyte diversity can be linked to human-associated RG development remains to be proven. Moreover, gliogenesis in the oSVZ seemingly take part in the expansion and gyrification of the primate cerebrum,[66] but the underlying regulating cellular mechanisms are still unclear. Here we have shown that the NES-Astro model captures several features of RG development and display astrocytic characteristics. In addition, the ltNES cells, the starting point of this model have shown robustness over multiple donors, both normal and disease models, as well as applicability to HTS settings. We suggest that the NES-Astro model can be used for detailed mechanistic studies of RG and astrocyte development under normal condition, as well as models of disease.

4. Experimental Section

Long Term Neural Epithelial Stem Cell Culture: It was previously shown that ltNES cells could be generated from several human iPSC and human embryonic stem cells (hESC) lines and that they could be cultured and maintain their neural stem cell profile for up to 100 passages.[9] Generation of ltNES cells from hiPSC was performed by the iPS Core facility at Karolinska Institutet by neural induction as previously described.[69] Stem cell cultures were lifted and by the use of collagenase (Invitrogen, Carlsbad, CA) dissociated into small aggregates and plated on ultra-low attachment plates in hESC media; DMEM/F12 or knock-out DMEM, 15% or 20% (KSR), 2 mM L-glutamine, 0.1 mM beta-mercaptoethanol, 0.1 mM NEAA (all from Invitrogen). Media was changed every second to third day for a period of 5–7 days. Plates were coated by applying 10 μg cm^{-2} poly-L-ornithine (Sigma, St. Louis, MO) diluted in phosphate-buffered saline (PBS) w. Ca/mg (Invitrogen) and floating aggregates were seeded into these plates. Rosettes, which

appear after about one week, were picked manually with a needle every second day. Before transferred to a non-adhesive culture plate the purity of the rosette clusters, later forming neurospheres, were visually inspected under the microscope assessing its morphology. After 2–5 days in DMEM/F12, 0.1 mg mL^{-1} penicillin/streptomycin, 1.6 g L^{-1} glucose, 2 mM L-glutamine, and N2 supplement (1:100; Invitrogen), neurospheres were dissociated in trypsin for 5–10 min before addition of a trypsin inhibitor. Cells were centrifuged for 5 min at 300 g before being resuspended and plated onto 2 μg cm^{-2} poly-L-ornithine and 0.2 μg cm^{-2} laminin (PLO-Laminin) (both Sigma) resuspended in PBS w. Ca/Mg (Invitrogen) coated plates into the same media supplemented with 10 ng mL^{-1} EGF, 10 ng mL^{-1} FGF2, (both from R&D systems, Minneapolis, MN), and B27 (1 μL mL^{-1}, Invitrogen). Every second to third day cells were passaged at a ratio of 1:3 using trypsin. Validation of the ltNES cell culture was validated by expression of Sox2, Nestin, PLZF, and ZO-1 (apical location in rosettes) as previously described.[9] Generation of ltNES cell lines had been performed previously (iPS Core at Karolinska Institutet) from human hiPSC lines AF22,[9] C1,[70] and C9,[71] which represented a variation in gender, age, and reprogramming techniques.

NES-Astro Differentiation: Long-term NES cells were plated at 60 000 cells cm^{-2} on 2 μg cm^{-2} poly-L-ornithine and 0.2 μg cm^{-2} laminin (PLO-Laminin) (Sigma, St. Louis, MO) double coated culture vessels in FHIA-differentiation medium; DMEM/F12, N2 supplement (1:100; Invitrogen, Carlsbad, CA), B27 (1:100; Invitrogen), FGF2 (8 ng mL^{-1}; PEPROTECH, Rocky Hill, NJ), heregulin 1β (10 ng mL^{-1}; Sigma), IGF1 (200 ng mL^{-1}; Sigma), activinA (10 ng mL^{-1}; PEPROTECH). The medium was changed every other day and cells were passaged once they reached 80% confluency; 7–9 passages during the differentiation protocol of 28 days. This was performed for ltNES cell lines AF22, C1, and C9 generating the NES-Astro phenotype for each line. Acquisition of RNA samples for long-RNA sequencing (>200 nt) was performed at day (d)0, d8, d15, d22, and d29. Additionally, in parallel to NES-Astro differentiation all ltNES cell lines were kept in maintenance culture[9] for the same period and sampled at the same timepoints to act as time specific normalization controls resulting in total of 81 RNA samples and n = 9 for each time point (Figure 1A). For small RNA sequencing ltNES cell line AF22 was sampled at day d0, d8, d15, d22, and d29 of NES-Astro differentiation. Proliferation during differentiation was assessed by estimation of doubling time via cell count using a Cedex HiRes Analyzer (Roche, Switzerland).

RNA Isolation: Total RNA was isolated using miRNeasy Kit according to the manufacturer's instructions (Qiagen). The quality of the RNA was assessed by a Fragment Analyzer (Advanced Analytical Technologies, Ankeny, IA). Samples with RNA integrity number >9 were used for library preparation. One microgram of total RNA was used for both long and small RNA library construction.

Long RNA Library Construction and Sequencing: Illumina TrueSeq Stranded mRNA LT Sample Prep Kit (Illumina, San Diego, CA) was used to construct poly(A) selected paired-end sequencing libraries according to TrueSeq Stranded mRNA Sample Preparation Guide (Illumina). All libraries were quantified with the Fragment Analyzer (Advanced Analytical Technologies), pooled and quantified with Qubit Fluorometer (Invitrogen), and sequenced using Illumina NextSeq 500 sequencer (Illumina). Three biological replicates were sequenced per sample.

Small RNA Library Construction, Sequencing: SMARTer smRNA-Seq kit for Illumina was used to micro RNA libraries according to Clontech Takara Bio Sample Preparation Guide. All libraries were quantified with the Fragment Analyzer (Advanced Analytical Technologies), pooled and quantified with Qubit Fluorometer (Invitrogen), and sequenced using Illumina NextSeq 500 sequencer (Illumina). Three biological replicates were sequenced per sample time point.

Immunocytochemistry: Immunocytochemistry and staining were carried out by fixating cells in formaldehyde for 10–20 min at room temperature. The fixated cells were washed 2× using PBS solution and incubated in blocking and permeabilization buffer; 10% donkey serum, 0.1% Triton X, PBS (all from Invitrogen), for 1 h at room temperature. Cells were directly washed 2× with PBS without incubation before adding

Table 1. Primary and secondary antibody specifications.

Antibody target	Species	Supplier	Cat. No.	Dilution
FABP7	Rabbit	Merck Millipore	ABN14	1:250
NF1A	Rabbit	Active Motif	39397	1:350
S100B	Mouse	Abcam	ab11179	1:500
SLC1A3 (EAAT1, Glast)	Mouse	Miltenyi Biotec	130-095-822	1:100
SLC1A2 (EAAT2, Glt1)	Rabbit	ThermoFish	701988	1:250
SOX9	Goat	R&D systems	AF3075	1:100
Isotype controls				
Isotype IgG1 mouse	Mouse	Life Technologies	02-6100	1:500
Isotype IgG rabbit	Rabbit	Life Technologies	10500C	1:1500
Isotype IgG goat	Goat	Life Technologies	02-6202	1:2500
Secondary antibodies				
Donkey anti-mouse IgG	Donkey	Life Technologies	A-21202	1:600
Donkey anti-rabbit IgG	Donkey	Life Technologies	A-10042	1:600
Donkey anti-goat IgG	Donkey	Life Technologies	A-21447	1:600

primary antibodies which were diluted in antibody buffer; 1% donkey serum, 0.01% triton, PBS (all from Invitrogen), and incubated at 4 °C overnight. Cells were directly washed 3× with PBS without incubation before addition of appropriate secondary antibodies in mono labeling or multiplexing. A 1 h incubation of the secondary antibody was performed followed by a 2× wash step without incubation using PBS. To stain cellular nuclei DAPI (1:2000; Invitrogen) was added for 10 min followed by a final 2× washing step without incubation using PBS before adding mounting medium, PBS. Primary and secondary antibodies used in the present study are presented in **Table 1**. Background signals were acquired using isotype controls matching the primary antibody. Images were captured using ImageXpress wide field microscope and downstream image analysis utilized MetaXpress software (both from Molecular Devices, Sunnyvale, CA).

Statistical Analysis: An overview of the RNAseq data was processed using Blue Collar Bioinformatics (bcbio-nextgen). The sequencing reads in fastq files were aligned to the human genome (hg38) via Hisat2, and read counts were extracted, summarized, and annotated using Sailfish and Htseq-count. The annotated, combined counts on gene level normalized to the control cell line were then used for differential expression analysis with the DESeq2[72] package for R (https://cran.r-project.org/) and for model based clustering. To first explore the data, a principal components analysis was performed on the DESeq2 rlog transformed data using R's base function prcomp.

Model-based clustering was performed (Mclust-R-package, http://www.stat.washington.edu/mclust/) which was based on a parametric finite mixture of Gaussian distributions and could be applied to time series/time-resolved data.[26] With this approach, each time series y_i, $i = 1,2,..., N$ (where $N = 5$ time points in the experiments reported in this study) was considered to be single entity connected by a line. Consequently, the data (in this case, all gene expression profiles within a given cell line) were assumed to be derived from a mixture of K underlying populations/groups, each corresponding to a cluster. This assumption transformed the clustering problem into a parameter estimation problem since the data could be modeled as a mixture of D component densities. Clustering was achieved by assigning each time series, y_i, to one of the K homogenous groups. The expectation–maximization (EM) algorithm computed the probabilities of assignment of each protein to each cluster (E step) and updated the cluster means and co-variances based on the set of proteins that belonged to that cluster (M-step). The Mclust-R package also calculated the Bayesian information criterion (BIC)[28] which expressed the likelihood that a set of multidimensional observations was described by a given model, p(X|Mk), where X represented the set of observations and Mk the model. The BIC was the value of the maximized log-likelihood with a penalty on the number of model parameters. In general, the lower the value of the BIC, the stronger the evidence for that particular model and number of clusters.[29]

The probabilistic (Gaussian mixture) model in Mclust had an advantage over other commonly used approaches because in this model the covariance structure (patterns in correlation matrices) accounted for correlation between abundance levels within an abundance profile. Thus, the model-based approach was more flexible than k-means or hierarchical clustering which commonly used just Euclidean distance.

Analysis of the miRNAome was done using a miraligner/isomiR package called SeqBuster.[73]

Gene set enrichment analysis was performed using a web-based tool called Enrichr which included 35 gene-set libraries. Enrichr computed enrichment score by Fisher's Exact test adjusting for multiple comparison providing an adjusted *p*-value ranking.[30,74]

Supporting Information

Supporting Information is available from the Wiley Online Library or from the author.

Acknowledgements

Conflict of Interest

The authors declare no conflict of interest.

**ADVANCED
SCIENCE NEWS**

www.advancedsciencenews.com

**ADVANCED
BIOSYSTEMS**

www.adv-biosys.com

[1] C. Dehay, H. Kennedy, K .S. Kosik, *Neuron* **2015**, *85*, 683.

[2] T. J. Nowakowski, A. A. Pollen, C. Sandoval-Espinosa, A. R. Kriegstein, *Neuron* **2016**, *91*,1219.

[3] T. Shimazaki, H. Okano, *npj Aging Mech. Dis.* **2016**, *2*, 15014.

[4] A. Lundin, L. Delsing, M. Clausen, P. Ricchiuto, J. Sanchez, A. Sabirsh, M. Ding, J. Synnergren, H. Zetterberg, G. Brolén, R. Hicks, A. Herland, A. Falk, *Stem Cell Rep.* **2018**, *10*, 1030.

[5] R. Krencik, J. P. Weick, Y. Liu, Z. J. Zhang, S. C. Zhang, *Nat. Biotechnol.* **2011**, *29*, 528.

[6] R. Santos, K. C. Vadodaria, B. N. Jaeger, A. Mei, S. Lefcochilos-Fogelquist, A. P. D. Mendes, G. Erikson, M. Shokhirev, L. Randolph-Moore, C. Fredlender, S. Dave, R. Oefner, C. Fitzpatrick, M. Pena, J. J. Barron, M. Ku, A. M. Denli, B. E. Kerman, P. Charnay, J. R . Kelsoe, M .C. Marchetto, F. H. Gage, *Stem Cell Rep.* **2017**, *8*, 1757.

[7] A. Serio, B. Bilican, S. J. Barmada, D. M. Ando, C. Zhao, R. Siller, K. Burr, G. Haghi, D. Story, A. L. Nishimura, M .A. Carrasco, H. P. Phatnani, C. Shum, I. Wilmut, T. Maniatis, C. E. Shaw, S. Finkbeiner, S. Chandran, *Proc. Natl. Acad. Sci. U.S.A.* **2013**, *110*, 4697.

[8] J. Tcw, M. Wang, A .A. Pimenova, K. R. Bowles, B. J. Hartley, E. Lacin, S. I. Machlovi, R. Abdelaal, C. M. Karch, H. Phatnani, P. A. Slesinger, B. Zhang, A. M. Goate, K. J. Brennand, *Stem Cell Rep.* **2017**, *9*, 600.

[9] A. Falk, P. Koch, J. Kesavan, Y. Takashima, J. Ladewig, M. Alexander, O. Wiskow, J. Tailor, M. Trotter, S. Pollard, A. Smith, O. Brustle, *PLoS One* **2012**, *7*, e29597.

[10] A. Kapusta, C. Feschotte, *Trends Genet.* **2014**, *30*,439.

[11] M. R. Freeman, D. H. Rowitch, *Neuron* **2013**, *80*, 613.

[12] M. Hawrylycz, J. A. Miller, V. Menon, D. Feng, T. Dolbeare, A. L. Guillozet-Bongaarts, A. G. Jegga, B. J. Aronow, C. K. Lee, A. Bernard, M. F. Glasser, D. L. Dierker, J. Menche, A. Szafer, F. Collman, P. Grange, K. A. Berman, S. Mihalas, Z. Yao, L. Stewart, A. L. Barabasi, J. Schulkin, J. Phillips, L. Ng, C. Dang, D. R. Haynor, A. Jones, D. C. Van Essen, C. Koch, E. Lein, *Nat. Neurosci.* **2015**, *18*, 1832.

[13] Y. Zhang, S. A. Sloan, L. E. Clarke, C. Caneda, C. A. Plaza, P. D. Blumenthal, H. Vogel, G. K. Steinberg, M. S. Edwards, G. Li, J. A. Duncan, 3rd, S. H. Cheshier, L. M. Shuer, E. F. Chang, G. A. Grant, M. G. Gephart, B. A. Barres, *Neuron* **2016**, *89*, 37.

[14] B. B. Lake, R. Ai, G. E. Kaeser, N. S. Salathia, Y. C. Yung, R. Liu, A. Wildberg, D. Gao, H. L. Fung, S. Chen, R. Vijayaraghavan, J. Wong, A. Chen, X. Sheng, F. Kaper, R. Shen, M. Ronaghi, J. B. Fan, W. Wang, J. Chun, K. Zhang, *Science* **2016**, *352*, 1586.

[15] X. Fan, J. Dong, S. Zhong, Y. Wei, Q. Wu, L. Yan, J. Yong, L. Sun, X. Wang, Y. Zhao, W. Wang, J. Yan, X. Wang, J. Qiao, F. Tang, *Cell Res.* **2018**, *28*, 730.

[16] N. A. Oberheim, S. A. Goldman, M. Nedergaard, *Methods Mol. Biol.* **2012**, *814*, 23.

[17] Z. He, D. Han, O. Efimova, P. Guijarro, Q. Yu, A. Oleksiak, S. Jiang, K. Anokhin, B. Velichkovsky, S. Grunewald, P. Khaitovich, *Nat. Neurosci.* **2017**, *20*, 886.

[18] D. Lanjakornsiripan, B.-J. Pior, D. Kawaguchi, S. Furutachi, T. Tahara, Y. Katsuyama, Y. Suzuki, Y. Fukazawa, Y. Gotoh, *Nat. Commun.* **2018**, *9*, 1623.

[19] A. A. Sosunov, X. Wu, N. M. Tsankova, E. Guilfoyle, G. M. McKhann, 2nd, J. E. G , *J. Neurosci.* **2014**, *34*, 2285.

[20] T. M. DeSilva, N. S. Borenstein, J. J. Volpe, H. C. Kinney, P. A. Rosenberg, *J. Comp. Neurol.* **2012**, *520*, 3912.

[21] V. T. Rao, S. K. Ludwin, S. C. Fuh, R. Sawaya, C. S. Moore, M. K. Ho, B. J. Bedell, H. B. Sarnat, A. Bar-Or, J. P. Antel, *J. Neuropathol. Exp. Neurol.* **2016**, *75*, 156.

[22] X. Han, M. Chen, F. Wang, M. Windrem, S. Wang, S. Shanz, Q. Xu, N. A. Oberheim, L. Bekar, S. Betstadt, A. J. Silva, T. Takano, S. A. Goldman, M. Nedergaard, *Cell Stem Cell.* **2013**, *12*, 342.

[23] Y. Sun, S. Pollard, L. Conti, M. Toselli, G. Biella, G. Parkin, L. Willatt, A. Falk, E. Cattaneo, A. Smith, *Mol. Cell. Neurosci.* **2008**, *38*, 245.

[24] J. Tailor, R. Kittappa, K. Leto, M. Gates, M. Borel, O. Paulsen, S. Spitzer, R. T. Karadottir, F. Rossi, A. Falk, A. Smith, *J. Neurosci.* **2013**, *33*, 12407.

[25] S. J. Liu, T. J. Nowakowski, A. A. Pollen, J. H. Lui, M. A. Horlbeck, F. J. Attenello, D. He, J. S. Weissman, A. R. Kriegstein, A. A. Diaz, D. A. Lim, *Genome Biol.* **2016**, *17*, 67.

[26] C. Bouveyron, C. Brunet-Saumard, *Comput. Stat. Data Anal.* **2014**, *71*, 52.

[27] G. J. McLachlan. 9 The classification and mixture maximum likelihood approaches to cluster analysis. in *Handbook of Statistics,* Vol 2, Elsevier B.V., **1982**. p. 199.

[28] G. Schwarz, *Ann. Stat.* **1978**, *6*, 461.

[29] C. Fraley, A. E. Raftery, *J. Am. Stat. Assoc.* **2002**, *97*, 611.

[30] M. V. Kuleshov, M. R. Jones, A. D. Rouillard, N. F. Fernandez, Q. Duan, Z. Wang, S. Koplev, S. L. Jenkins, K. M. Jagodnik, A. Lachmann, M. G. McDermott, C. D. Monteiro, G. W. Gundersen, A. Ma'ayan, *Nucleic Acids Res.* **2016**, *44*, W90.

[31] S. A. Fietz, R. Lachmann, H. Brandl, M. Kircher, N. Samusik, R. Schroder, N. Lakshmanaperumal, I. Henry, J. Vogt, A. Riehn, W. Distler, R. Nitsch, W. Enard, S. Paabo, W. B. Huttner, *Proc. Natl. Acad. Sci. USA* **2012**, *109*, 11836.

[32] J. A. Miller, S. Horvath, D. H. Geschwind, *Proc. Natl. Acad. Sci. USA.* **2010**, *107*, 12698.

[33] A. A. Pollen, T. J. Nowakowski, J. Chen, H. Retallack, C. Sandoval-Espinosa, C. R. Nicholas, J. Shuga, S. J. Liu, M. C. Oldham, A. Diaz, D. A. Lim, A. A. Leyrat, J. A. West, A. R. Kriegstein, *Cell* **2015**, *163*, 55.

[34] A. A. Pollen, T. J. Nowakowski, J. Shuga, X. Wang, A. A. Leyrat, J. H. Lui, N. Li, L. Szpankowski, B. Fowler, P. Chen, N. Ramalingam, G. Sun, M. Thu, M. Norris, R. Lebofsky, D. Toppani, D. W. Kemp, 2nd, M. W , B. Clerkson, B. N. Jones, S. Wu, L. Knutsson, B. Alvarado, J. Wang, L. S. Weaver, A. P. May, R. C. Jones, M. A. Unger, A. R. Kriegstein, J. A. West, *Nat. Biotechnol.* **2014**, *32*, 1053.

[35] Z. Yao, J. K. Mich, S. Ku, V. Menon, A. R. Krostag, R. A. Martinez, L. Furchtgott, H. Mulholland, S. Bort, M. A. Fuqua, B. W. Gregor, R. D. Hodge, A. Jayabalu, R. C. May, S. Melton, A. M. Nelson, N. K. Ngo, N. V. Shapovalova, S. I. Shehata, M. W. Smith, L. J. Tait, C. L. Thompson, E. R. Thomsen, C. Ye, I .A. Glass, A. Kaykas, S. Yao, J. W. Phillips, J. S. Grimley, B .P. Levi, Y. Wang, S. Ramanathan, *Cell Stem Cell.* **2017**, *20*, 120.

[36] E. R. Thomsen, J. K. Mich, Z. Yao, R. D. Hodge, A. M. Doyle, S. Jang, S. I. Shehata, A. M. Nelson, N. V. Shapovalova, B. P. Levi, S. Ramanathan, *Nat. Methods.* **2016**, *13*, 87.

[37] M. B. Johnson, P. P. Wang, K. D. Atabay, E. A. Murphy, R. N. Doan, J. L. Hecht, C. A. Walsh, *Nat. Neurosci.* **2015**, *18*, 637.

1900226 (12 of 13)

[38] J. M. Spaethling, Y. J. Na, J. Lee, A. V. Ulyanova, G. H. Baltuch, T. J. Bell, S. Brem, H. I. Chen, H. Dueck, S. A. Fisher, M. P. Garcia, M. Khaladkar, D. K. Kung, T. H. Lucas, Jr., D. M. O'Rourke, D. Stefanik, J. Wang, J. A. Wolf, T. Bartfai, M. S. Grady, J. Y. Sul, J. Kim, J. H. Eberwine, *Cell Rep.* **2017**, *18*, 791.

[39] S. Darmanis, S. A. Sloan, Y. Zhang, M. Enge, C. Caneda, L. M. Shuer, M. G. Hayden Gephart, B. A. Barres, S. R. Quake, *Proc. Natl. Acad. Sci. USA* **2015**, *112*, 7285.

[40] P. Kang, H. K. Lee, S. M. Glasgow, M. Finley, T. Donti, Z. B. Gaber, B. H. Graham, A. E. Foster, B. G. Novitch, R. M. Gronostajski, B. Deneen, *Neuron* **2012**, *74*, 79.

[41] X. Li, Y. Tao, R. Bradley, Z. Du, Y. Tao, L. Kong, Y. Dong, J. Jones, Y. Yan, C. R. K. Harder, L. M. Friedman, M. Bilal, B. Hoffmann, S.-C. Zhang, *Stem Cell Rep.* **2018**, *11*, 998.

[42] I. Canals, A. Ginisty, E. Quist, R. Timmerman, J. Fritze, G. Miskinyte, E. Monni, M. G. Hansen, I. Hidalgo, D. Bryder, J. Bengzon, H. Ahlenius, *Nat. Methods.* **2018**, *15*, 693.

[43] J. Tchieu, E. L. Calder, S. R. Guttikonda, E. M. Gutzwiller, K. A. Aromolaran, J. A. Steinbeck, P. A. Goldstein, L. Studer, *Nat. Biotechnol.* **2019**, *37*, 267.

[44] S. Magavi, D. Friedmann, G. Banks, A. Stolfi, C. Lois, *J. Neurosci.* **2012**, *32*, 4762.

[45] J. A. Briggs, E. J. Wolvetang, J. S. Mattick, J. L. Rinn, G. Barry, *Neuron* **2015**, *88*, 861.

[46] M. Rajman, G. Schratt, *Development* **2017**, *144*, 2310.

[47] H. Naka-Kaneda, T. Shimazaki, H. Okano, *Neurogenesis* **2014**, *1*, e29542.

[48] M. Patterson, X. Gaeta, K. Loo, M. Edwards, S. Smale, J. Cinkornpumin, Y. Xie, J. Listgarten, S. Azghadi, S. M. Douglass, M. Pellegrini, W. E. Lowry, *Stem Cell Rep.* **2014**, *3*, 758.

[49] A. Shenoy, M. Danial, R. H. Blelloch, *EMBO J.* **2015**, *34*, 1180.

[50] G. P. Meares, R. Rajbhandari, M. Gerigk, C. L. Tien, C. Chang, S. C. Fehling, A. Rowse, K. C. Mulhern, S. Nair, G. K. Gray, N. F. Berbari, M. Bredel, E. N. Benveniste, S. E. Nozell, *Glia* **2018**, *66*, 987.

[51] Y.-B. Ouyang, L. Xu, S. Liu, R. G. Giffard, *Adv. Neurobiol.* **2014**, *11*, 171.

[52] R. Edri, Y. Yaffe, M. J. Ziller, N. Mutukula, R. Volkman, E. David, J. Jacob-Hirsch, H. Malcov, C. Levy, G. Rechavi, I. Gat-Viks, A. Meissner, Y. Elkabetz, *Nat. Commun.* **2015**, *6*, 6500.

[53] M. Nagao, T. Ogata, Y. Sawada, Y. Gotoh, *Nat. Commun.* **2016**, *7*, 11102.

[54] L .C. deAzevedo, C. Fallet, V. Moura-Neto, C. Daumas-Duport, C. Hedin-Pereira, R. Lent, *J. Neurobiol.* **2003**, *55*, 288.

[55] X. Li, J. M. Newbern, Y. Wu, M. Morgan-Smith, J. Zhong, J. Charron, W. D. Snider, *Neuron* **2012**, *75*, 1035.

[56] X. Heng, Q. Guo, A. W. Leung, J. Y. Li, *eLife* **2017**, *6*, e23253.

[57] N. Rani, T. J. Nowakowski, H. Zhou, S. E. Godshalk, V. Lisi, A. R. Kriegstein, K. S. Kosik, *Neuron* **2016**, *90*, 1174.

[58] H. T. Ghashghaei, J. M. Weimer, R. S. Schmid, Y. Yokota, K. D. McCarthy, B. Popko, E. S. Anton, *Genes Dev.* **2007**, *21*, 3258.

[59] R. S. Schmid, B. McGrath, B. E. Berechid, B. Boyles, M. Marchionni, N. Sestan, E. S. Anton, *Proc. Natl. Acad. Sci. USA* **2003**, *100*, 4251.

[60] A. Sharif, V. Prevot, *Neurochem. Int.* **2010**, *57*, 344.

[61] S. A. Sloan, S. Darmanis, N. Huber, T. A. Khan, F. Birey, C. Caneda, R. Reimer, S. R. Quake, B. A. Barres, S. P. Pasca, *Neuron* **2017**, *95*, 779.

[62] T. J. Nowakowski, N. Rani, M. Golkaram, H. R. Zhou, B. Alvarado, K. Huch, J. A. West, A. Leyrat, A. A. Pollen, A. R. Kriegstein, L. R. Petzold, K. S. Kosik, *Nat. Neurosci.* **2018**, *21*, 1784.

[63] A. A. Pollen, A. Bhaduri, M. G. Andrews, T. J. Nowakowski, O. S. Meyerson, M. A. Mostajo-Radji, E. Di Lullo, B. Alvarado, M. Bedolli, M. L. Dougherty, I. T. Fiddes, Z. N. Kronenberg, J. Shuga, A. A. Leyrat, J. A. West, M. Bershteyn, C. B. Lowe, B. J. Pavlovic, S. R. Salama, D. Haussler, E. E. Eichler, A. R. Kriegstein, *Cell* **2019**, *176*, 743.

[64] M. Caiazzo, S. Giannelli, P. Valente, G. Lignani, A. Carissimo, A. Sessa, G. Colasante, R. Bartolomeo, L. Massimino, S. Ferroni, C. Settembre, F. Benfenati, V. Broccoli, *Stem Cell Rep.* **2015**, *4*, 25.

[65] D. V. Hansen, J. H. Lui, P. R. L. Parker, A .R. Kriegstein, *Nature* **2010**, *464*, 554.

[66] B. G. Rash, A. Duque, Y. M. Morozov, J. I. Arellano, N. Micali, P. Rakic. **2019**, *116*, 7089.

[67] J. Steiner, H.-G. Bernstein, H. Bielau, A. Berndt, R. Brisch, C. Mawrin, G. Keilhoff, B. Bogerts, *BMC Neurosci.* **2007**, *8*, 2.

[68] N. A. Oberheim, T. Takano, X. Han, W. He, J. H. Lin, F. Wang, Q. Xu, J. D. Wyatt, W. Pilcher, J. G. Ojemann, B. R. Ransom, S. A. Goldman, M. Nedergaard, *J. Neurosci.* **2009**, *29*, 3276.

[69] P. Koch, T. Opitz, J. A. Steinbeck, J. Ladewig, O. Brustle, *Proc. Natl. Acad. Sci. U.S.A.* **2009**, *106*, 3225.

[70] M. Shahsavani, R. J. Pronk, R. Falk, M. Lam, M. Moslem, S. B. Linker, J. Salma, K. Day, J. Schuster, B. M. Anderlid, N. Dahl, F. H. Gage, A. Falk, *Mol. Psychiatry.* **2018**, *23*, 1674.

[71] E. Uhlin, H. Ronnholm, K. Day, M. Kele, K. Tammimies, S. Bolte, A. Falk, *Stem Cell Res.* **2017**, *18*, 22.

[72] M. I. Love, W. Huber, S. Anders, *Genome Biol.* **2014**, *15*, 550.

[73] L. Pantano, X. Estivill, E. Marti, *Nucleic Acids Res.* **2010**, *38*, e34.

[74] E. Y. Chen, C. M. Tan, Y. Kou, Q. Duan, Z. Wang, G. V. Meirelles, N. R. Clark, A. Ma'ayan, *BMC Bioinformatics* **2013**, *14*, 128.